Available online at www.sciencedirect.com
SCIENCE DIRECT
Journal of Power Sources 153 (2006) 385–390
JOURNAL OF POWER SOURCES
www.elsevier.com/locate/jpowsour

Short communication

SEI film formation on highly crystalline graphitic materials in lithium-ion batteries

H. Buqa [a,*], A. Würsig [a], J. Vetter [a], M.E. Spahr [b], F. Krumeich [c], P. Novák [a]

[a] *Paul Scherrer Institut, Electrochemistry Laboratory, CH-5232 Villigen PSI, Switzerland*
[b] *TIMCAL SA, CH-6743 Bodio, Switzerland*
[c] *Swiss Federal Institute of Technology, Laboratory of Inorganic Chemistry, CH-8093 Zurich, Switzerland*

Available online 12 July 2005

Abstract

In situ differential electrochemical mass spectrometry (DEMS) was used to study the SEI film formation on highly crystalline TIMREX® SLX50 graphite negative electrodes during the first electrochemical lithium insertion using either 1 M $LiPF_6$ in ethylene carbonate (EC) with either dimethyl carbonate (DMC) or propylene carbonate (PC) as co-solvent. In the case of the propylene and ethylene carbonate containing electrolyte, DEMS measurements indicate strong formation of ethylene and propylene gas below 0.75 V versus Li/Li^+, which does not decrease at lower cell potential and in the subsequent charge/discharge cycles. Whereas for the dimethyl carbonate containing electrolyte, ethylene gas formation could be observed already above 1 V versus Li/Li^+. *Post mortem* scanning electron microscopy (SEM) studies of the electrodes show strong exfoliation of the graphite electrode when they are discharged in the ethylene/propylene carbonate electrolyte, indicating the formation of an unstable SEI layer. The addition of vinylene carbonate (VC) as a film forming additive significantly decreases the gas formation at the graphite electrode in the propylene carbonate containing electrolyte. The exfoliation was suppressed by the vinylene carbonate additive. We show that the combination of different in situ and ex situ methods can provide new useful information about the passivation process of graphite, as well as the solid electrolyte interphase layer formed, during the first electrochemical insertion of lithium into graphite negative electrode materials.

Keywords: Lithium-ion cell; Graphite electrode; SEI film; Additive; In situ DEMS; Post mortem SEM

1. Introduction

In lithium-ion batteries with either liquid or gelled polymer electrolytes, a passivating layer called the solid electrolyte interphase (SEI) [1,2] is formed during the first charge. The SEI layer suppresses, if the film forming process is optimised, any further electrolyte decomposition and avoids the exfoliation of the graphite structure [1–4]. At the same time, it allows the passage lithium ions. Thus, the SEI is the key component in the negative electrode determining the electrochemical performance and safety of the whole lithium-ion battery. However, the mechanism of its formation is rather complex and not yet completely understood.

A thorough understanding of the chemistry and morphology of this interphase layer is crucial for an improvement of the cell performance. In recent years, there have been numerous investigations of SEI-related phenomena and this field is an ongoing topic of research. Besenhard et al. [5] proposed that the SEI film is formed through the co-intercalation of solvent molecules, along with the Li^+ ions, into the graphite host. However, an alternative formation mechanism of SEI formation was also proposed. According to this model, the SEI is formed by the decomposition of electrolytes on the graphite surface [6,7]. For the formation of an effective SEI layer, both, the electrolyte composition and the material bulk and surface properties of the graphite material play an important role [5–12]. It is necessary to understand the individual influences of structural defects (rhombohedral stacking faults) and surface defects on the irreversible charge capacity (often called

* Corresponding author.
E-mail address: hilmi.buqa@psi.ch (H. Buqa).

0378-7753/$ – see front matter © 2005 Elsevier B.V. All rights reserved.
doi:10.1016/j.jpowsour.2005.05.036

"charge loss"). The identification of the material parameters that influence the SEI formation will be an important achievement for facilitating further improvements of carbon negative electrode materials for lithium-ion batteries [13–20].

In commonly used electrolytes such as 1 M $LiPF_6$ in ethylene carbonate (EC)/dimethyl carbonate (DMC), the irreversible charge loss occurring during the first reduction depends linearly on the specific BET surface area of the graphite material used [2,18]. On the other hand, many graphite-based negative materials are not able to intercalate lithium-ions reversibly in propylene carbonate (PC)-based electrolytes. It is known that most graphitic materials with high crystallinity show exfoliation during the first electrochemical insertion of lithium in propylene carbonate. This graphite exfoliation results in an enhanced irreversible charge loss and reduced cycling stability [21–23] and, thus, in battery failure. The graphite exfoliation can be avoided if propylene carbonate is replaced by its non-substituted cyclic carbonate homologue, ethylene carbonate [4,10,11]. So, in the EC/PC, $LiPF_6$ mixture, striking differences can be observed in the SEI film formation depending on the type of graphite used. One way to avoid the exfoliation of graphite is the use of electrolyte additives. Among them, vinylene carbonate (VC) is a well investigated substance that is able to form a stable polymer film at the graphite surface prior to the electrochemical reduction of the main solvents [24].

The complex interaction between the graphite electrode and the electrolyte makes the analysis of the SEI layer highly challenging. We are confident that by combining various in situ and ex situ techniques, a sufficient basic knowledge to understand these processes can be acquired. We employed different techniques as in situ DEMS and *post mortem* SEM along with classical electrochemical charge/discharge tests.

2. Experimental

As active anode material, either TIMREX® SLX50 (TIMCAL Ltd., Bodio, Switzerland) graphite (specific BET surface area: 4 $m^2\,g^{-1}$) powder, or an experimental graphite powder which is further denoted graphite A (specific BET surface area: 5 $m^2\,g^{-1}$) was used as received. Electrodes were prepared by blade-coating the graphite on a copper foil. 10 wt.% polyvinylidene difluoride (SOLEF 1015, Solvay SA) was used as binder. The electrolyte solvents EC, PC and DMC, as well as the conducting salts $LiPF_6$ and $LiClO_4$ had battery quality (Selectipur®, E. Merck, Darmstadt, Germany) and were used as received.

The electrochemical charge/discharge measurements were carried out at 25 (±0.1) °C in hermetically sealed laboratory test cells [25] using a computer controlled cell capture system (CCCC, Astrol Electronic AG, Oberrohrdorf, Switzerland). The coin-cell type laboratory test cells with an electrode area of 1.33 cm^2 were assembled in an argon-filled glove box with a content of <1 ppm of both, H_2O and O_2. A cell consisted of: (i) a graphite working electrode, (ii) a 1 mm thick soft glass-fibre separator (type EUJ116, Hollingsworth & Vose Ltd., England) soaked with 500 μl electrolyte and (iii) a 0.75 mm thick lithium foil (Alfa Aaesar, Johnson Matthey GmbH, Germany, purity 99.9%) as counter and reference electrode. The cell components were put under a light pressure with a spring (pressure ca. 2 kg cm^{-2}). The working electrodes and the relevant parts of the cells were dried under vacuum at 120 °C for 16 h. The water content of the electrolytes was less than 10 ppm.

Unless otherwise stated, the galvanostatic measurements were performed at specific currents of 10 mA g^{-1} of carbon to complete the SEI formation in the first Li^+ insertion cycle. After a potential of 5 mV versus Li/Li^+ was reached, the charging[1] was continued potentiostatically until the specific current dropped below 5 mA g^{-1}. The same constant current/constant voltage (CCCV) profile was applied during lithium de-intercalation with a cut-off potential of 1.5 V versus Li/Li^+.

The electrodes for the *post mortem* scanning electron microscopy (SEM) studies were first galvanostatically charged at 10 mA g^{-1} to 0.3 V versus Li^+, and were then equilibrated for 48 h at this potential as described elsewhere [19]. Scanning electron microscopy (SEM) was performed on a LEO 1530 Gemini microscope, which was operated at low voltage (usually 1 kV) to achieve a suitable contrast of the surface details in the secondary electron images and to minimise charging of the uncoated samples. Powders were dispersed in ethanol and deposited on a conducting tape, whereas the electrodes were mounted on stubs.

DEMS was used to study the process of electrolyte decomposition and SEI formation, and to follow the formation of different gaseous reaction products on the graphite electrodes during the first electrochemical reduction. The DEMS setup has been described elsewhere [26]. Depending on the electrolyte, various gases such as ethylene, propylene, hydrogen and carbon dioxide (CO_2) can be detected. The method is based on the non-wettability of a porous membrane that acts as a solvent barrier between the electrochemical cell and the vacuum system of the mass spectrometer. A porous working electrode, which was prepared using a spray technique, is deposited onto the membrane. The active mass of the electrodes was about 4 mg cm^{-2}. The membrane is the critical component of the DEMS cell; it has to minimise the evaporation of the low-boiling electrolyte components while remaining sufficiently permeable for the volatile reaction products. Therefore, we introduced a second PTFE-based membrane, which can be adapted to different experimental conditions by heat treatment. The gaseous reaction products are pumped off continuously through the membranes during the electrochemical reaction, and are analysed on line with a quadrupole mass spectrometer. Hence, intensity changes in mass signals can be detected as a function of time and/or potential and,

[1] Terminology related to processes in full cells is used throughout the manuscript.

thus, can be correlated with current peaks in the cyclic voltammogram or plateaus in the galvanostatic charge/discharge curves. The measurement cell was assembled inside the glove box using 2 ml of electrolyte and a lithium metal counter and reference electrode. The DEMS measurements presented here were carried out potentiodynamically at room temperature using a scan rate of 0.4 mV s^{-1} between 2 and 0.01 V versus Li/Li^+. The current (cyclic voltammogram, CV) and mass signals (mass spectrometric cyclic voltammogram, MSCV) were recorded simultaneously as functions of the electrode potential.

3. Results and discussion

Fig. 1 shows the different electrochemical response in the first galvanostatic lithium insertion/de-insertion in TIMREX® SLX50 graphite in 1 M $LiPF_6$, EC/DMC 1/1 (w/w) and 1 M $LiPF_6$, EC/PC 1/1 (w/w) as electrolyte system. In EC/DMC, SLX50 graphite shows the typical insertion properties expected for a highly crystalline graphite material. The short plateau or shoulder at ca. 0.8 V versus Li/Li^+ (see arrow in Fig. 1, bottom) corresponds to the SEI film formation process. A reversible capacity of about 360 mAh g^{-1} with a coulombic efficiency of 94% could be observed at a specific current of 10 mA g^{-1}. In contrast, the higher reduction potential at ca. 0.9 V versus Li/Li^+ and a very large additional plateau observed in the case of the EC/PC electrolyte (see arrow in Fig. 1, top) indicates that a different reduction mechanism occurs in this electrolyte and leads to graphite exfoliation [5,19]. Various factors directly and indirectly affect the potential of this additional plateau. Up to now, it was challenging to determine the parameters which influence this phenomenon.

From the electrochemical results, we can clearly see that the different SEI film formation depends on the electrolyte used. To further investigate the film formation behaviour on the graphite negative electrode in different electrolytes, we performed post mortem SEM studies of SLX50 graphite on electrodes which were galvanostatically charged to 0.3 V versus Li/Li^+, and subsequently stabilised potentiostatically at this potential. Fig. 2 (top) shows the SEM picture of uncycled SLX50 graphite. The graphene layers are well ordered and compact, without expanded distances. Fig. 2 (bottom) displays the effect of exfoliation of the same graphite, electrochemically reduced in EC/PC. The separation gap between the graphene layers has greatly increased and at some points

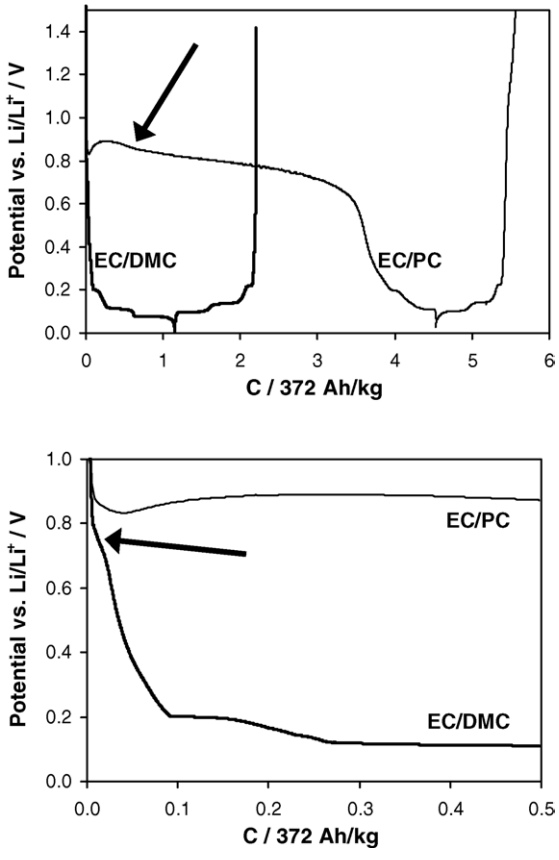

Fig. 1. (Top) First electrochemical intercalation/de-intercalation of lithium into/from TIMREX® SLX50 in 1 M $LiPF_6$, EC/DMC 1/1 (w/w) and in 1 M $LiPF_6$, EC/PC 1/1 (w/w) as electrolyte at a specific current of 10 mA g^{-1}. An enlarged part of the diagram (bottom).

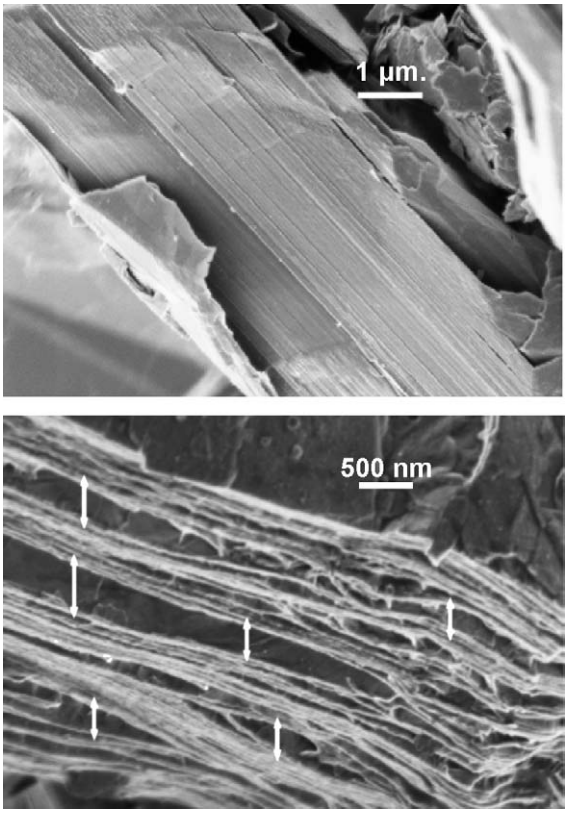

Fig. 2. (Top) SEM image of TIMREX® SLX50 powder graphite material and (bottom) *post mortem* SEM image of a SLX50 graphite negative electrode taken from a half-cell. The electrode was charged galvanostatically at 10 mA g^{-1} to 0.3 V vs. Li/Li^+ and stabilised potentiostatically at this potential for 2 days using 1 M $LiPF_6$ in EC/PC 1/1 (w/w) as electrolyte. In this case, heavy exfoliation can be observed (arrows).

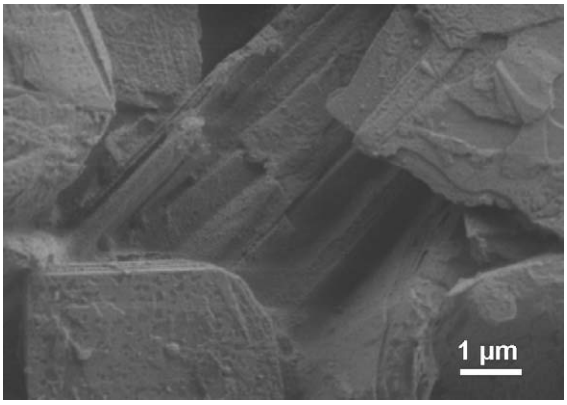

Fig. 3. *Post mortem* SEM images of a TIMREX® SLX50 graphite negative electrode taken from a half-cell. The electrode was charged galvanostatically at 10 mA g^{-1} to 0.3 V vs. Li/Li^+ and stabilised potentiostatically at this potential for 2 days using 1 M $LiPF_6$ in EC/DMC 1/1 (w/w) as electrolyte.

big caverns have arisen (arrows in Fig. 2, bottom). This supports the hypothesis that electrochemical graphite exfoliation is caused by the co-intercalation of solvents, along with the Li^+ ions, between the graphite layers during the film formation, followed by the decomposition of the solvent molecules (as suggested by Besenhard et al. [5]).

To obtain an even clearer picture about the role of the electrolyte on the film formation, we performed *post mortem* SEM studies of SLX50 electrodes stabilised in 1 M $LiPF_6$, EC/DMC electrolyte. In this case, no exfoliation of the graphene layers can be observed. A very uniform SEI film is covering the entire graphite surface (Fig. 3).

In our previous work, we have shown that the exfoliation process could also be identified by post mortem XRD studies of an electrode from a half-cell which was charged to 0.3 V versus Li/Li^+ and stabilised at this potential [19]. Furthermore, DEMS measurements were performed to investigate the consequences of the graphite exfoliation on the SEI formation. During the exfoliation, the formation of ethylene, propylene and hydrogen was observed. These gases were used to monitor the graphite passivation and film formation process.

Wagner et al. [27] have found that the failure of graphite electrodes in the pure PC electrolyte may be related to gas formation inside the graphite. In the case of the EC/DMC electrolye, ethylene and hydrogen gas could be detected during the first electrochemical insertion of lithium in SLX50, as shown in Fig. 4. Besides, non-volatile products, which cannot be detected by the DEMS method, are deposited on the electrode surface as shown previously [24]. Ethylene formation starts from potentials positive to 1 V versus Li/Li^+ with a maximum at 0.53 V versus Li/Li^+. The ethylene mass signal diminishes with decreasing potentials to almost zero. A significantly weaker ethylene mass signal is detected in the second cycle with a maximum at 0.90 V versus Li/Li^+ indicating that the formation of the passivation layer is achieved. Surprisingly, the evolution of hydrogen starts at a potential of about 1 V versus Li/Li^+ in the first cycle, and a higher amount

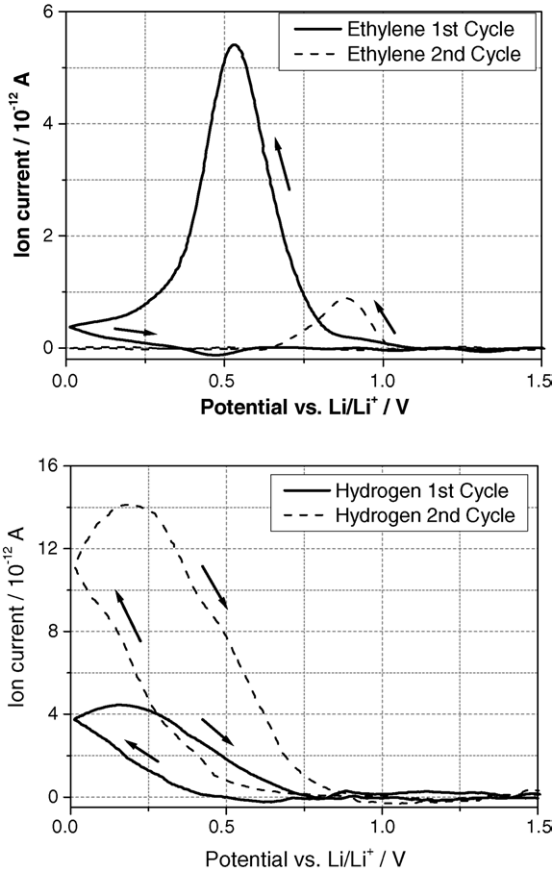

Fig. 4. DEMS measurements in TIMREX® SLX50 in 1 M $LiPF_6$, EC/DMC 1/1 (w/w) electrolyte. Mass signals corresponding to (top) ethylene ($m/z = 27$) and (bottom) hydrogen ($m/z = 2$), respectively, are shown. The gas formation was monitored as a function of the potential applied to the graphite electrode at a scan rate of 0.4 mV s^{-1} (MSCV mode).

of hydrogen is detected in the second cycle (Fig. 4, bottom). In the following cycles, the evolution of hydrogen decreases rapidly (not shown in this paper).

Using 1 M $LiPF_6$, EC/PC as electrolyte, apart from the formation of ethylene and hydrogen, propylene gas could be detected in the mass spectrometer. Both, the ethylene and propylene formation start at a similar potential of about 0.80 V versus Li/Li^+ and the gas evolution is continuous until a potential of 0.01 V versus Li/Li^+ is reached (Fig. 5, top). This indicates that the formation of a stable passivation film was hindered. The gas formation can be observed even during the next cycles (not shown) between 0.90 and 0.01 V versus Li/Li^+ indicating, thus, that the passivation film is still not complete. In contrast to the evolution of ethylene and propylene, the evolution of hydrogen starts at a potential of about 2 V versus Li/Li^+ in the first cycle, and a small amount of hydrogen can also be observed in the second cycle (Fig. 5, bottom). Interestingly, the maximum of the hydrogen formation shown in Fig. 5, bottom, appears at a potential of about 0.75 V versus Li/Li^+, at which the graphite exfoliation process starts. The gas formation at the graphite electrode during the first reduction in the EC/PC electrolyte significantly dif-

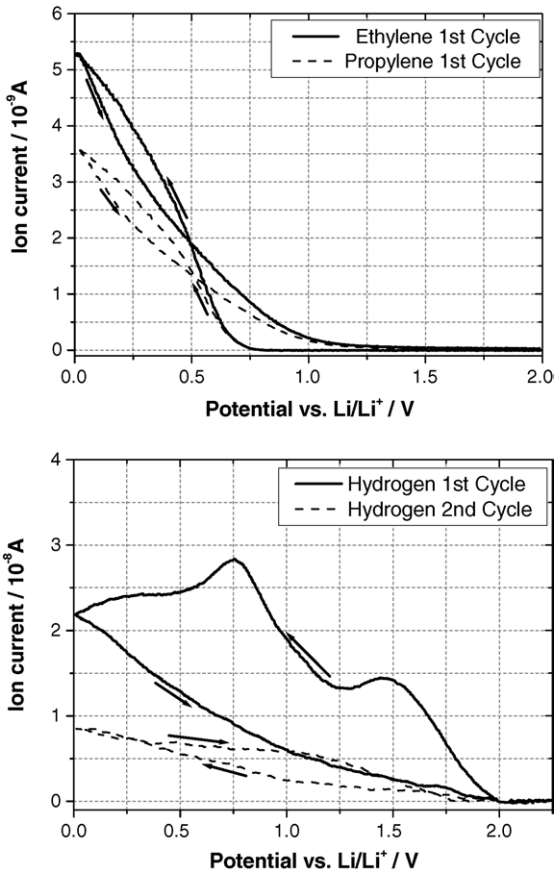

Fig. 5. DEMS measurements in TIMREX® SLX50 in 1 M $LiPF_6$, EC/PC 1/1 (w/w) electrolyte. Mass signals corresponding to (top) ethylene ($m/z = 27$), propylene ($m/z = 41$) and (bottom) hydrogen ($m/z = 2$), respectively, are shown. The gas formation was monitored as a function of the potential applied to the graphite electrode at a scan rate of 0.4 mV s^{-1} (MSCV mode).

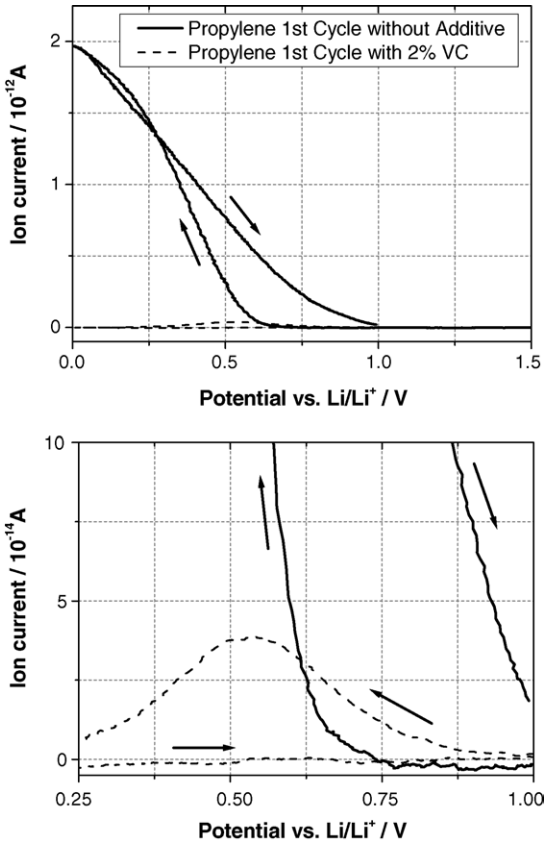

Fig. 6. (Top) DEMS measurements in half-cells with graphite A vs. metallic Li in 1 M $LiPF_6$, EC/PC 1/1 (w/w) electrolyte without and with 2% VC as additive. The mass signal corresponds to propylene ($m/z = 41$). The gas formation was monitored as a function of the potential applied to the graphite electrode at a scan rate of 0.4 mV s^{-1} (MSCV mode). An enlarged part of the diagram (bottom).

fers to the EC/DMC electrolyte system. These results demonstrate that PC has a different electrochemical reactivity on the graphite surface than EC and acyclic carbonates [19]. The decomposition products of solvated graphite intercalation compounds formed upon the reduction in EC/PC electrolytes are not able to form an effective SEI. This provides space for further solvent co-intercalation and the electrochemical exfoliation of the graphite.

An elegant method to hinder exfoliation of graphite is the addition of film forming compounds to the electrolyte. Among these electrolyte additives, vinylene carbonate is known to be very effective and in forming a stable passivation layer at the graphite electrode surface which is even stable at elevated temperatures [28]. In order to study the impact of this additive, the experimental graphite A was chosen for its pronounced tendency to exfoliate. With this challenging system, the influence of the additive becomes most obvious.

For both, the VC containing and the VC free electrolyte system, propylene, ethylene and hydrogen could be detected as volatile compounds in the DEMS measurement. The huge impact of VC on the propylene gas evolution at graphite A electrode in 1 M $LiPF_6$, EC/PC electrolyte can be seen in Fig. 6. In the electrolyte without VC additive, a strong propylene signal starting at about 0.75 V versus Li/Li^+, indicates the graphite exfoliation by electrolyte co-intercalation and decomposition. The reductive electrolyte degradation takes place until the lower potential limit of 0.01 V is reached, showing that the exfoliation process is not yet finished, and the propylene gas formation continues in the second cycle. If 2% VC is added to the electrolyte, only a marginal amount of propylene is formed. This gas evolution also starts at a more positive potential of about 0.90 V versus Li/Li^+. The figures for ethylene formation are not shown here but follow the same trend. One can assume that the film created by the polymerisation of VC (caused by an electrochemical process which takes place at about 1.2 V versus Li/Li^+ [24]) passivates the graphite surface and avoids further electrolyte decomposition and the exfoliation of the graphite structure. It might also be possible that the film formed by VC reduction also provides new reaction sites for the electrolyte reduction, which is now no longer hindered by the low surface reactivity of the graphite. As a result, the SEI formation is completed prior to the beginning of graphite exfoliation. The SEI is

stable and prevents graphite exfoliation during the following cycles. As can be seen from the DEMS results, besides the formation of an efficient solid electrolyte interphase, the addition of VC also decreases the amount of gassing which occurs during the graphite passivation and film formation.

4. Conclusion

The SEI formation on graphite is a complex electrochemical surface reaction which can be influenced by many factors. The differences in electrolyte decomposition and passivation mechanisms of graphite in different electrolytes indicate that the nature of the electrolyte has an essential impact on the formation and composition of the SEI layer. In EC/PC-based electrolytes, electrochemical exfoliation can be observed. When VC is used as an additive, the SEI formation is completed prior to the beginning of exfoliation. To obtain an efficient passivation and high-quality SEI film on the surface of the graphite negative electrode material, the electrolyte composition needs to be adjusted to the graphite material. *Post mortem* SEM and DEMS analyses are suitable methods for the investigation of the SEI.

Acknowledgements

The authors wish to thank the Swiss National Science Foundation and the Swiss Federal Office of Education and Science for financial support.

References

[1] E. Peled, J. Electrochem. Soc. 126 (1979) 2047.
[2] M. Winter, J.O. Besenhard, M.E. Spahr, P. Novak, Adv. Mater. 10 (1998) 725.
[3] E. Peled, in: G.P. Gabano (Ed.), Lithium Batteries, Academic Press, New York, 1983, p. 43.
[4] E. Peled, D. Golodnitsky, J. Penciner, in: J.O. Besenhard (Ed.), Handbook of Battery Materials, Wiley-VCH, New York, 1999 (Chapter 6).
[5] J.O. Besenhard, M. Winter, J. Yang, W. Biberacher, J. Power Sources 54 (1995) 228.
[6] D. Aurbach, M.D. Levi, E. Levi, A. Schechter, J. Phys. Chem. B 101 (1997) 2195.
[7] E. Peled, D. Golodnitsky, C. Menachem, D. Bar-Tow, J. Electrochem. Soc. 145 (1998) 3482.
[8] A.N. Dey, B.D. Sullivan, J. Electrochem. Soc. 117 (1970) 222.
[9] M. Inaba, Z. Siroma, Y. Kawaate, A. Funabiki, Z. Ogumi, J. Power Sources 68 (1997) 221.
[10] J.R. Dahn, A.K. Sleigh, H. Shi, B.M. Way, W.J. Weydanz, J.N. Reimers, Q. Zhong, U. von Sacken, in: G. Pistoia (Ed.), Lithium Batteries, New Materials, Developments and Perspectives, Elsevier, Amsterdam, 1994, pp. 1–47 (Chapter 1).
[11] R. Fong, U. von Sacken, J.R. Dahn, J. Electrochem. Soc. 137 (1990) 2009.
[12] D. Aurbach, B. Markovsky, I. Weissman, E. Levi, Y. Ein-Eli, Electrochim. Acta 45 (1999) 67.
[13] H. Buqa, P. Golob, M. Winter, J.O. Besenhard, J. Power Sources 97–98 (2001) 122.
[14] F. Cao, I.V. Barsukov, H.J. Bang, P. Zalesky, J. Prakash, J. Electrochem. Soc. 147 (2000) 3579.
[15] R. Yazami, Electrochim. Acta 45 (1999) 87.
[16] F. Kong, R. Kostecki, G. Nadeau, X. Song, K. Zaghib, K. Kinoshita, F. McLarnon, J. Power Sources 97–98 (1998) 58.
[17] H. Huang, W. Liu, X. Huang, L. Chen, E.M. Kelder, J. Schoonman, Solid State Ionics 110 (1998) 173.
[18] F. Joho, B. Rykart, A. Blome, P. Novák, H. Wilhelm, M.E. Spahr, J. Power Sources 97–98 (2001) 78.
[19] M.E. Spahr, T. Palladino, H. Wilhelm, A. Würsig, D. Goers, H. Buqa, M. Holzapfel, P. Novák, J. Electrochem. Soc. 151 (2004) A1383.
[20] R.S. McMillan, M.W. Juskow, J. Electrochem. Soc. 138 (1991) 1556.
[21] D. Aurbach, B. Markovsky, A. Shechter, Y. Ein-Eli, H. Cohen, J. Electrochem. Soc. 143 (1996) 3809.
[22] K. Guerin, A. Fevrier-Bouvier, S. Flandrois, M. Couzi, B. Simon, P. Biensan, J. Electrochem. Soc. 146 (1999) 3660.
[23] M.E. Spahr, H. Wilhelm, F. Joho, J.-C. Panitz, J. Wambach, P. Novák, N. Dupont-Pavlovsky, J. Electrochem. Soc. 149 (2002) A960.
[24] D. Aurbach, K. Gamolsky, B. Markovsky, Y. Gofer, M. Schmidt, U. Heider, Electrochim. Acta 47 (2003) 1423.
[25] P. Novák, W. Scheifele, F. Joho, O. Haas, J. Electrochem. Soc. 142 (1995) 2544.
[26] R. Imhof, P. Novák, J. Electrochem. Soc. 145 (1998) 1081.
[27] M.R. Wagner, P.R. Raimann, A. Trifonova, K.-C. Möller, J.O. Besenhard, M. Winter, J. Anal. Bioanal. Chem. 379 (2004) 272.
[28] M. Inaba, T. Uno, A. Tasaka, 12th International Meeting on Lithium Batteries (IMLB-12), Nara, Japan, 2004 (Abstr. 262).